


 Cite this: *RSC Adv.*, 2023, **13**, 10642

TiO₂/porous carbon as a new nanocomposite and catalyst for the preparation of 4*H*-pyrimido[2,1-*b*]benzimidazoles†

 Zahra Jalilian,^a Ahmad Reza Moosavi-Zare,^{ID *b} Mohammad Ghadermazi,^{ID *a} and Hamid Goudarziafshar^b

A nano TiO₂/porous carbon nanocomposite (TiO₂/PCN) was designed by the pyrolysis of peanut shells as bio waste with nano titanium dioxide. In the presented nanocomposite, titanium dioxide is properly placed in the positions and pores of the porous carbon, so that it acts as an optimal catalyst in the nanocomposite structure. The structure of TiO₂/PCN was studied by various analyses such as Fourier transform infrared spectroscopy (FT-IR), energy-dispersive X-ray Spectroscopy (EDX), scanning electron microscopy (SEM), SEM coupled EDX (SEM mapping), transmission electron microscopy (TEM), X-ray fluorescence (XRF) and BET. TiO₂/PCN was successfully tested as a nano catalyst for the preparation of some 4*H*-pyrimido[2,1-*b*]benzimidazoles in high yields (90–97%) and short reaction times (45–80 min).

 Received 17th January 2023
 Accepted 28th March 2023

DOI: 10.1039/d3ra00367a

rsc.li/rsc-advances

1. Introduction

4*H*-pyrimido[2,1-*b*]benzazoles including 4*H*-pyrimido[2,1-*b*]benzimidazole derivatives are important heterocyclic compound derivatives and are used in the structure of various drugs due to some significant biological activities such as anti-inflammatory,¹ anti-tumor,² anti-bacterial³ and anti-fungal properties.⁴

One of the important strategies for the preparation of 4*H*-pyrimido[2,1-*b*]benzimidazoles is the multi-component condensation reaction of A β-keto ester with various aldehydes and 2-aminobenzimidazole.⁵ The multi-component reaction is an important strategy for the synthesis of organic compounds due to preparing the main product in one step, without the formation of side products. Preventing the loss of energy, materials and solvent are some other advantages of this protocol.^{6–13}

Multi-component synthesis of 4*H*-pyrimido[2,1-*b*]benzazoles was reported using various catalysis such as, nano-[Co-4CSP] Cl₂,⁵ iron fluoride,¹⁴ Fe₃O₄@nano-cellulose/TiCl₃,¹⁵ chitosan,¹⁶ nano-Fe₃O₄@SiO₂-TiCl₃,¹⁷ H₃PO₄-Al₂O₃,¹⁸ nano-TiCl₂/cellulose,¹⁹ acetic acid,²⁰ TMGT,²¹ 1,3-disulfonic acid imidazolium trifluoroacetate,²² [bmim]BF₄,²³ GO@PSA-Cu²⁴ and poly (vinyl-pyrrolidonium) perchlorate.²⁵ Due to importance of 4*H*-pyrimido[2,1-*b*]benzimidazoles, the find of the more efficient

method for the preparation of these significant compounds are still needed.

Millions of tons of biomass waste annually are produced as renewable materials in the world. These wastes can be created from the remains of plants or animals. Low price, low density, ability to return to the environment, good electrical conductivity, easy pyrolysis and degradable structure are important advantages of this category of waste materials.^{26–30} One of the biggest renewable sources of carbon is biomass, which is cheap and widely accessible.^{31,32} Peanut shell is one of the important agricultural wastes, which due to its easy pyrolysis, low density and high fiber content, is a suitable template and precursor for the production of porous carbon with a high effective surface. Placing metal oxides and other functional groups in the porous carbon substrate causes chemical activation and its high catalytic ability in promoting chemical reactions.³³

Peanut shell as bio-waste material was successfully used for the design of various catalysts which applied in different chemical process such as cycloaddition of epoxides with CO₂,³³ degradation of organic pollutant,³⁴ production aromatic rich monomer compounds,³⁵ synthesis of 5-hydroxymethylfurfural from glucose, fructose, cellulose and agricultural wastes,³⁶ esterification of cyclohexene with formic acid³⁷ and synthesis of 1,2,3-triazoles.³⁸

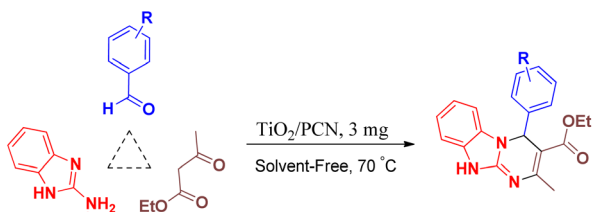
Herein, we have used peanut shell as bio-waste for the preparation of porous carbon as a template for the placement of nano titanium dioxide on it to give TiO₂/porous carbon nanocomposite (TiO₂/PCN). TiO₂/PCN as a novel and efficient heterogeneous catalyst was successfully used for the preparation of 4*H*-pyrimido[2,1-*b*]benzimidazoles (Scheme 1).

^aDepartment of Chemistry, University of Kurdistan, P.O. Box 66135-416, Sanandaj, Iran. E-mail: mghadermazi@yahoo.com

^bDepartment of Chemical Engineering, Hamedan University of Technology, Hamedan, 65155, Iran. E-mail: moosavizare@yahoo.com

† Electronic supplementary information (ESI) available. See DOI: <https://doi.org/10.1039/d3ra00367a>





Scheme 1 The preparation of 4*H*-pyrimido[2,1-*b*]benzimidazoles using TiO₂/PCN.

2. Results and discussion

In this work, we have used peanut shell to prepare the porous carbon according the previous literature.³¹ In this regard, peanut shell as bio-waste material was crushed, burned and then, mixed with nano TiO₂ in the mass ratio 3 : 1. This

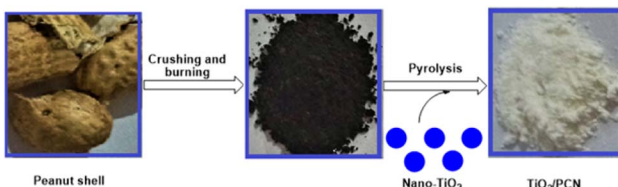


Fig. 1 Preparation steps of TiO₂/porous carbon nanocomposite (TiO₂/PCN).

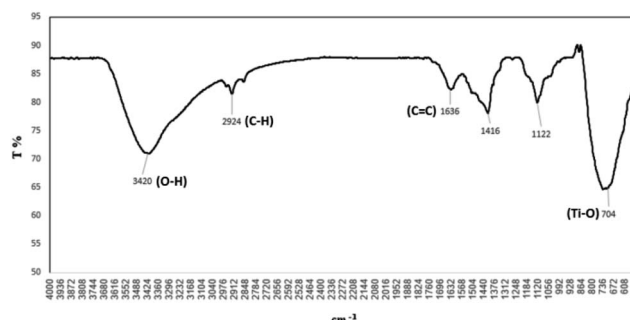


Fig. 2 FT-IR spectrum of TiO₂/PCN.

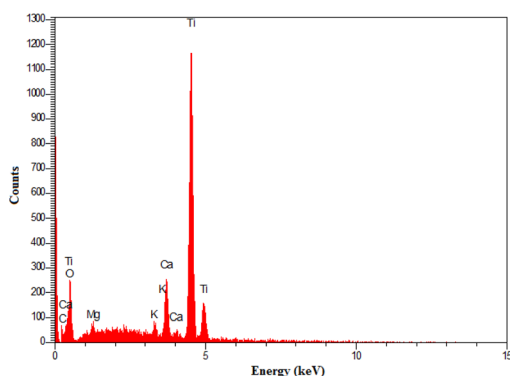


Fig. 3 Energy-dispersive X-ray spectroscopy (EDX) of TiO₂/PCN.

presented mixture was heated in 600 °C for 6 hours to prepare TiO₂/porous carbon nanocomposite (TiO₂/PCN). TiO₂/PCN was prepared by pyrolysis of peanut shell with nano TiO₂ in rutile form (Fig. 1). This composite was structured in nano size and

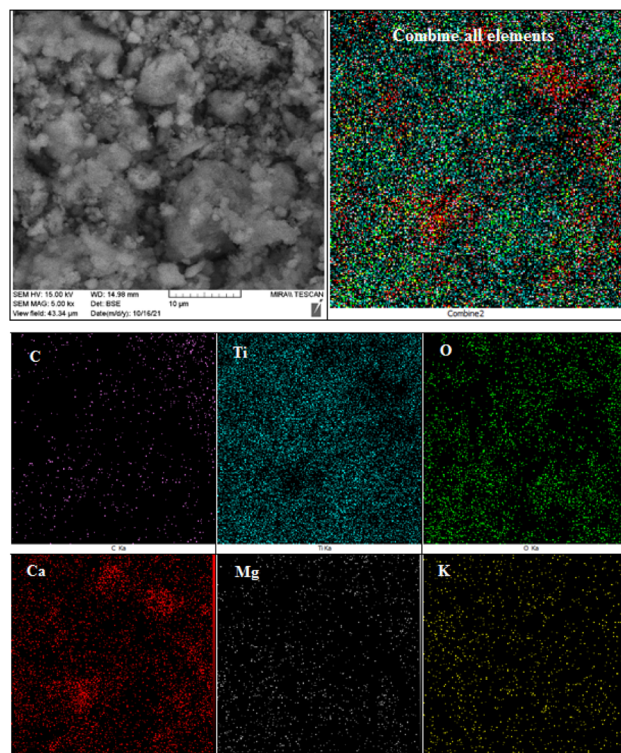


Fig. 4 SEM coupled EDX (SEM mapping) of TiO₂/PCN.

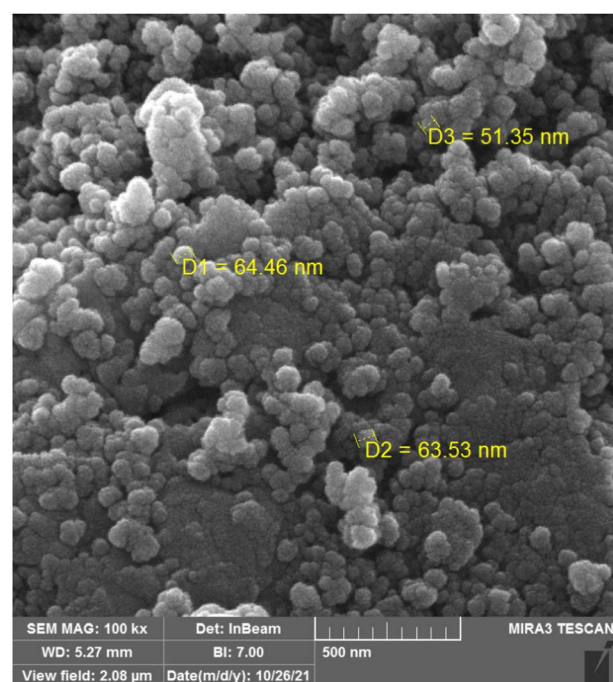


Fig. 5 SEM micrograph of TiO₂/PCN.



dispersed in the surface of porous carbon with high and effective surface and large volume which could be applied as an efficient catalyst in organic synthesis.

FT-IR spectrum of TiO_2/PCN was studied and a broad peak appeared at $3500\text{--}3600\text{ cm}^{-1}$ which could be related to vibration of the O-H bonds from hydroxyl groups.³⁷ Another peak at 1636 cm^{-1} is belonged to C=C bond vibrations of the carbon skeleton^{39,40} (Fig. 2). FT-IR spectrum of TiO_2 was compared with TiO_2/PCN . The images were given in ESI† (Fig. S1).

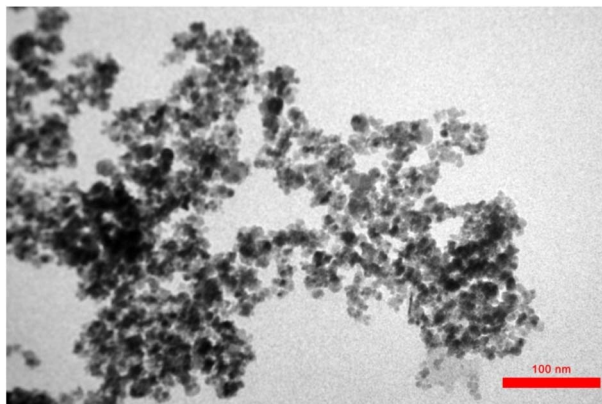


Fig. 6 TEM micrograph of TiO_2/PCN .

Table 1 Specific surface area (SBET), mean pore diameter and total pore volume of TiO_2/PCN

Sample	Specific surface area ($\text{m}^2 \text{ g}^{-1}$)	Mean pore diameter (nm)	Total pore volume ($\text{cm}^3 \text{ g}^{-1}$)
TiO_2/PCN	60.151	30.848	0.4639

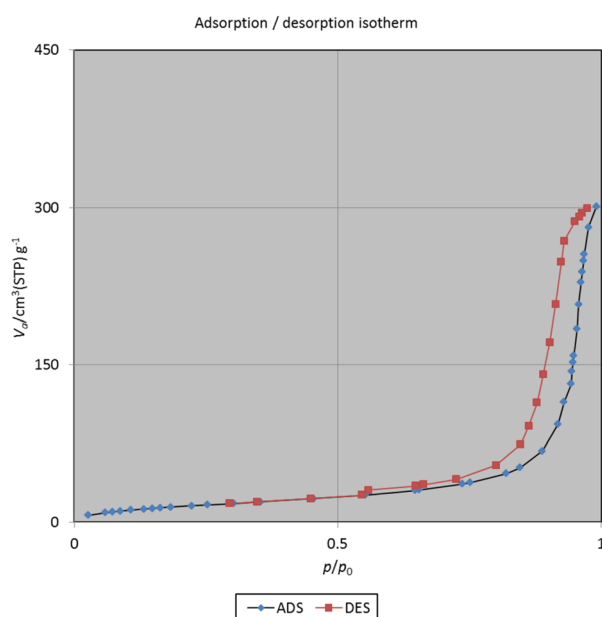


Fig. 7 N_2 adsorption–desorption isotherms of TiO_2/PCN .

Table 2 The effect of temperature, amount of catalyst and solvents on the model reaction

Entry	Catalyst (mg)	Solvent	Temperature (°C)	Time (min)	Yield ^a (%)
1	TiO_2/PCN (1)	—	90	60	74
2	TiO_2/PCN (3)	—	90	60	95
3	TiO_2/PCN (6)	—	90	60	95
4	(—)	—	90	60	19
5	TiO_2/PCN (3)	—	25	60	—
6	TiO_2/PCN (3)	—	50	60	43
7	TiO_2/PCN (3)	—	70	60	95
8	TiO_2/PCN (3)	—	100	60	95
9	TiO_2/PCN (3)	<i>n</i> -Hexane	Reflux	60	16
10	TiO_2/PCN (3)	Dichloromethane	Reflux	60	54
11	TiO_2/PCN (3)	Ethyl acetate	Reflux	60	71
12	TiO_2/PCN (3)	Ethanol	Reflux	60	95
13	TiO_2 (3)	—	70	60	25
14	PCN (3)	—	70	60	5

^a Isolated yields.



Table 3 The preparation of 4*H*-pyrimido[2,1-*b*]benzimidazoles

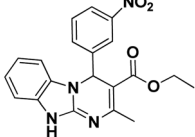
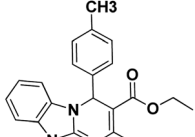
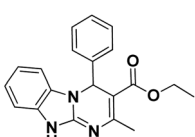
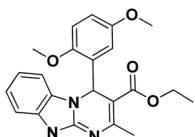
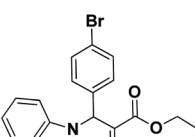
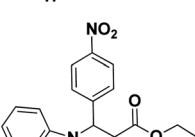
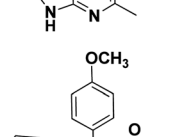
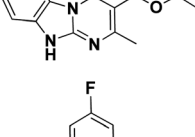
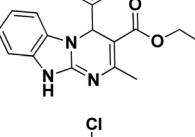
Entry	Product	Time (min)	Yield ^a (%)	M.p °C (Lit.) ^{ref}
1		65	97	293–295 (291–292) ⁵
2		75	92	258–260 (261–263) ²²
3		65	95	290–292 (294–296) ²³
4		70	90	255–258
5		65	94	304–306 (>300) ²³
6		45	95	298–300 (>300) ²³
7		80	80	258–260 (256–258) ²⁵
8		75	87	307–309 (>300) ²³
9		60	95	308–310 (302–303) ⁴¹



Table 3 (Contd.)

Entry	Product	Time (min)	Yield ^a (%)	M.p °C (Lit.) ^{ref}
10		65	97	245–247 (250–252) ²⁴
11		70	95	315–318 (>300) ⁴¹
12		75	95	261–263

^a Isolated yield.

The presented elements in TiO_2/PCN were investigated by energy-dispersive X-ray spectroscopy (EDX) (Fig. 3). From the examination of Fig. 3, it is clear that the desired elements such as carbon, oxygen, titanium and other elements in the peanut shell structure namely calcium, magnesium and potassium were also observed in the prepared nanocomposite.

In the next investigation, the distribution of the elements in the prepared nanocomposite structure was investigated and studied by SEM mapping analysis (Fig. 4). As it is found from the Fig. 4, indicates that, the elements of carbon, titanium, oxygen and to a lesser amount potassium, calcium and magnesium are distributed well in the nanocomposite structure.

Types of elemental oxides in the nanocomposite structure determined by X-ray fluorescence (XRF) analysis. The results were obtained in Fig. S2 in ESI[†]

The morphology and the particle size of TiO_2/PCN were investigated by scanning electron microscopy (SEM) (Fig. 5). As it is shown in Fig. 5, indicates that the presented particles from TiO_2/PCN , were prepared in size less than 100 nanometers (Fig. 5).

The size of the prepared nanocomposite was also investigated by transmission electron microscopy (TEM). According that, as it is displayed from Fig. 6, demonstrated that the particles of TiO_2/PCN were obtained in nano size.

Because of the porous structure of catalyst particles, to show the effective surface of complex to catalyze the reactions, the volume and size of the cavities included in TiO_2/PCN nanocomposite were studied. The specific surface area, mean pore diameter and total pore volume of TiO_2/PCN nanocomposite are

60.151 $\text{m}^2 \text{ g}^{-1}$, 30.848 nm and 0.4639 $\text{cm}^3 \text{ g}^{-1}$ respectively (Table 1 and Fig. 7).

To find the best reaction condition, at first the reaction of 2-aminobenzimidazole, 4-chlorobenzaldehyde and ethyl acetoacetate was selected as a model reaction and various conditions such as amount of catalyst, temperature, kinds of solvent vs. solvent-free condition were examined on this reaction. After this investigation, the best yield and short reaction time were obtained in the presence of 3 mg of the catalyst at 70 °C under solvent-free condition. The model reaction was also tested in the absence of catalyst which the yield of the obtained product was not suitable (Table 2). To show the efficiency of the prepared nanocomposite as a catalyst in comparison with the moieties in its structure, nano titanium dioxide and porous carbon were separately tested on the model reaction which the obtained results were not better than the main catalyst. The obtained results from these reactions were given in Table 2. Moreover, various allotropes of titanium dioxide namely rutile and anatase used in the structure of nanocomposite and tested on the model reaction which the prepared composite with nano titanium dioxide in rutile form was more effective than anatase form to catalyze the reaction (Table 2).

After the optimization of the reaction condition, to investigate the generality and the efficiency of the catalyst, various aldehydes containing electron-releasing groups, electron-withdrawing groups and halogens on the aromatic ring were reacted with ethyl acetoacetate and 2-aminobenzothiazole to give 4*H*-pyrimido[2,1-*b*]benzimidazoles in high yields and short reaction times. The obtained results were given in Table 3.



In a suggested mechanism, which is supported by the literature,^{5–25,41} ethyl acetoacetate reacted with aldehyde which is activated by TiO_2/PCN to prepare intermediate (I). Then, 2-aminobenzimidazole is reacted with intermediate (I) to give (II). In the next step, by the intramolecular nucleophilic attack to carbonyl group in intermediate (II) which is activated by TiO_2/PCN , intermediate (III) is generated. Finally, by removing of one molecule of H_2O from (III), the desired product is obtained (Scheme 2).

The reusability of TiO_2/PCN as a nanocomposite and catalyst was also tested on the reaction of 2-aminobenzimidazole, 4-chlorobenzaldehyde and ethyl acetoacetate. After the completion of the reaction, the reaction mixture was extracted by warm ethanol and separated from the catalyst by simple filtration. The separated catalyst was washed with ethyl acetate, dried and successfully reused for four times (Fig. 8). The FT-IR of reused

catalyst in comparison with fresh catalyst was given in Fig. S3 in ESI.†

The catalytic ability of the new nanocomposite is increased due to the distribution of nano titanium dioxide in the porous carbon support and the increase in the surface of the catalyst in comparison with the porous carbon and titanium dioxide separately. Using peanut shell as biological waste is important and economical in designing the structure of this nanocomposite.

3. Conclusions

In summary, $\text{TiO}_2/\text{porous carbon nanocomposite} (\text{TiO}_2/\text{PCN})$ was prepared by the pyrolysis of peanut shell, as bio-waste and green material, with nano titanium dioxide in rutile form. TiO_2/PCN was fully studied by various techniques including FT-IR, EDX, SEM mapping, SEM, TEM, BET and XRF analyses. TiO_2/PCN was successfully used as an efficient and reusable heterogeneous catalyst for the preparation of some 4*H*-pyrimido[2,1-*b*]benzimidazoles.

4. Experimental

4.1. Procedure for the synthesis of TiO_2/PCN

Peanut shells were crushed and ground in a mortar and then burned. Then, burnt peanut shell (0.075 g) was mixed with nano titanium dioxide (0.025 g) in rutile form. The presented mixture was placed in the oven and heated for 6 hours at 600 °C to produce TiO_2/PCN nanocomposite.

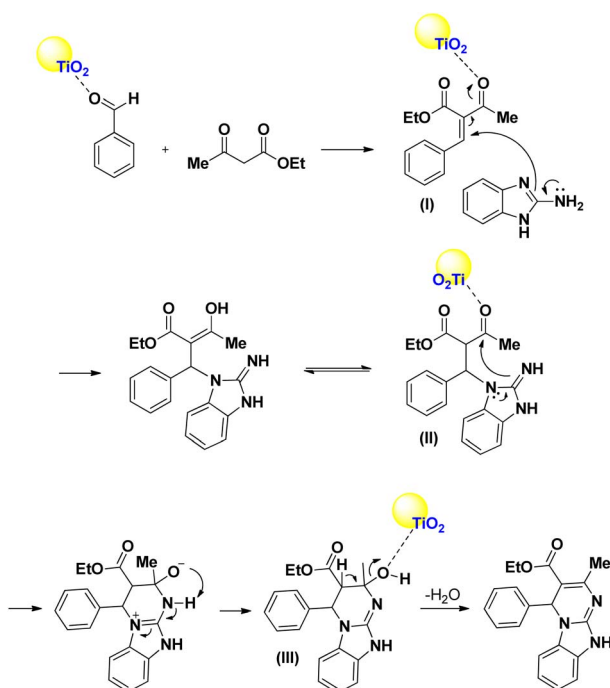
4.2. General procedure for the synthesis of 4*H*-pyrimido[2,1-*b*]benzimidazoles

A mixture of aromatic aldehyde, (1 mmol), ethyl acetoacetate (1 mmol, 0.13 g), 2-aminobenzimidazole (1 mmol, 0.133 g) and TiO_2/PCN nanocomposite (3 mg) as a catalyst was added to 25 mL round-bottomed flask connected to a reflux condenser and stirred at 70 °C under solvent-free conditions. After the completion of the reaction, as monitored by TLC, the reaction mixture was extracted with warm ethanol (10 mL) and separated from the catalyst by simple filtration. Finally, the desired product was purified by the recrystallization in ethanol (90%).

4.3. Selected spectral data of compounds

4.3.1 Ethyl 2-methyl-4-(*p*-tolyl)-4,10-dihydrobenzo[4,5]imidazo[1,2-*a*]pyrimidine-3-carboxylate (2). Yellow solid; M.p: 258–260 °C; yield: 92%; IR (KBr, cm^{-1}): 3238, 3162, 3106, 2934, 1698, 1659, 1621, 852, 474; $^1\text{H-NMR}$: (250 MHz, $\text{DMSO-}d_6$): δ (ppm) 1.12 (t, J = 7.50 Hz, 3H), 2.43 (s, 3H), 3.62 (s, 3H), 3.98 (q, J = 7.50 Hz, 2H), 6.35 (s, 1H), 6.77 (d, J = 7.50 Hz, 2H), 6.88–7.04 (m, 2H), 7.20–7.33 (m, 4H), 10.77, (s, 1H); $^{13}\text{CNMR}$: (62.5 MHz, $\text{DMSO-}d_6$): δ (ppm); 14.5, 19.0, 55.3, 55.7, 59.7, 98.6, 110.3, 114.0, 117.1, 120.5, 122.1, 128.7, 131.9, 134.6, 142.7, 146.0, 146.5, 159.0, 165.6.

4.3.2 Ethyl 4-(2,5-dimethoxyphenyl)-2-methyl-4,10-dihydrobenzo[4,5]imidazo[1,2-*a*]pyrimidine-3-carboxylate (4). Yellow solid; M.p: 255–258 °C; yield: 90%; IR (KBr, cm^{-1}): 3231,



Scheme 2 The proposed mechanism for the synthesis of 4*H*-pyrimido[2,1-*b*]benzimidazoles.

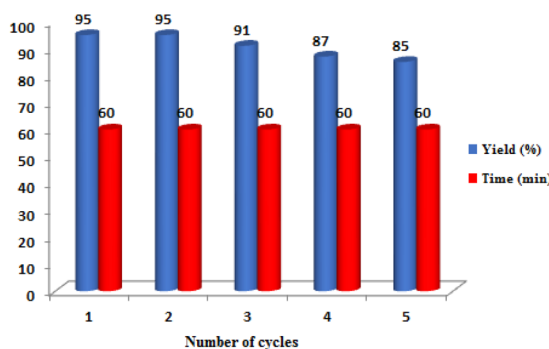


Fig. 8 The recovery of TiO_2/PCN .



3100, 3170, 2974, 2839, 1658, 1617, 1575, 828 701; $^1\text{H-NMR}$: (250 MHz, DMSO- d_6): δ (ppm) 1.07 (t, J = 7.50 Hz, 3H), 2.43 (s, 3H), 3.61 (s, 3H), 3.70 (s, 3H), 3.94 (q, J = 7.50 Hz, 2H), 6.58 (s, 1H), 6.72 (d, J = 7.50 Hz, 1H), 6.83 (d, J = 7.50 Hz, 2H), 6.91–7.02 (m, 2H), 7.29 (d, J = 7.50, 1H), 10.74 (s, 1H); $^{13}\text{CNMR}$: (62.5 MHz, DMSO- d_6): δ (ppm); 14.3, 18.9, 51.7, 55.6, 56.4, 59.5, 96.8, 109.7, 112.8, 113.5, 115.5, 117.0, 120.4, 121.9, 130.9, 132.2, 142.6, 146.3, 147.4, 151.1, 153.3, 165.6.

4.3.3 Ethyl 4-(3-chlorophenyl)-2-methyl-4,10-dihydrobenzo[4,5]imidazo[1,2-*a*]pyrimidine-3-carboxylate (10). Yellow solid; M.p: 245–247 °C; yield: 97%; IR (KBr, cm^{-1}): 3275, 3258, 32, 19, 3090, 2955, 1661, 1642, 1606, 844, 529; $^1\text{H-NMR}$: (250 MHz, DMSO- d_6): δ (ppm) 1.12 (t, J = 7.50 Hz, 3H), 2.44 (s, 3H), 4.00 (t, J = 7.5 Hz, 2H), 6.43 (s, 1H), 9.91–7.06 (m, 2H), 7.24–7.35 (m, 5H), 7.44 (s, 1H), 10.89 (s, 1H); $^{13}\text{CNMR}$: (62.5 MHz, DMSO- d_6): δ (ppm); 14.4, 19.1, 55.7, 59.8, 97.7, 110.2, 117.3, 120.7, 122.3, 126.0, 127.5, 128.2, 130.8, 131.8, 133.2, 142.6, 144.8, 145.8, 147.4, 165.4.

4.3.4 Ethyl 4-(4-(benzyloxy)phenyl)-2-methyl-4,10-dihydrobenzo[4,5]imidazo[1,2-*a*]pyrimidine-3-carboxylate. Yellow solid; M.p: 261–263 °C; yield: 95%; IR (KBr, cm^{-1}): 3238, 3106, 3034, 2980, 1697, 1617, 1510, 830, 696; $^1\text{H-NMR}$: (250 MHz, DMSO- d_6): δ (ppm) 1.11 (t, J = 7.50 Hz, 3H), 2.43 (s, 3H), 3.98 (q, J = 7.50 Hz, 2H), 4.95 (s, 2H), 6.35 (s, 1H), 6.84–7.04 (m, 5H), 7.21–7.34 (m, 8H), 10.79 (s, NH); $^{13}\text{CNMR}$: (62.5 MHz, DMSO- d_6): δ (ppm); 14.5, 19.0, 55.7, 59.7, 69.6, 98.5, 110.3, 114.8, 117.1, 120.5, 122.1, 128.1, 128.2, 128.7, 128.8, 131.9, 134.8, 137.3, 142.7, 146.0, 146.6, 158.2, 165.6.

Conflicts of interest

There are no conflicts to declare.

Acknowledgements

We thank the Hamedan University of Technology and University of Kurdistan, for financial support to our research group.

Notes and references

1. S. Nalawade, V. Deshmukh and S. Chaudhari, *J. Pharm. Res.*, 2013, **7**, 433.
2. M. T. Gabr, N. S. El-Gohary, E. R. El-Bendary and M. M. El-Kerdawy, *Eur. J. Med. Chem.*, 2014, **85**, 576.
3. P. H. Tran, T.-P. T. Bui, X.-Q. B. Lam and X.-T. T. Nguyen, *RSC Adv.*, 2018, **8**, 36392.
4. M. S. Chaitanya, G. Nagendrappa and V. P. Vaidya, *J. Chem. Pharm. Res.*, 2010, **2**, 206.
5. A. R. Moosavi-Zare, H. Goudarziafshar and P. Fashi, *Res. Chem. Intermed.*, 2020, **46**, 5567.
6. A. Khazaei, A. R. Moosavi-Zare, H. Afshar-Hezarkhani and V. Khakyzadeh, *Eurasian Chem. Commun.*, 2020, **2**, 27.
7. A. R. Moosavi-Zare and H. Afshar-Hezarkhani, *Eurasian Chem. Commun.*, 2020, **2**, 465.
8. A. R. Moosavi-Zare, H. Goudarziafshar, Z. Jalilian and F. Hosseinabadi, *Chem. Methodol.*, 2022, **6**, 571.
9. A. Khazaei, F. Gohari-Ghalil, M. Tavasoli, M. Rezaei-Gohar and A. R. Moosavi-Zare, *Chem. Methodol.*, 2020, **4**, 543.
10. N. Irandejad-Gheshlaghchaei, A. Zare, A. Banaei, H. Kaveh and N. Varavi, *Chem. Methodol.*, 2020, **4**, 400.
11. M. A. Zolfigol, S. Baghery, A. R. Moosavi-Zare and S. M. Vahdat, *J. Mol. Catal. A: Chem.*, 2015, **409**, 216.
12. A. Khazaei, H. A. Alavi Nik and A. R. Moosavi-Zare, *J. Chin. Chem. Soc.*, 2015, **62**, 675.
13. A. R. Moosavi-Zare, M. A. Zolfigol, E. Noroozizadeh, O. Khaledian and B. Shirmardi Shaghaseemi, *Res. Chem. Intermed.*, 2016, **42**, 4759.
14. A. B. Atar, Y. S. Jeong and Y. T. Jeong, *Tetrahedron*, 2014, **70**, 5207.
15. S. Azad and B. B. F. Mirjalili, *RSC Adv.*, 2016, **6**, 96928.
16. P. K. Sahu, P. K. Sahu, S. K. Gupta and D. D. Agarwal, *Ind. Eng. Chem. Res.*, 2014, **53**, 2085.
17. S. A. Fazeli-Attar and B. B. Fatameh Mirjalili, *Res. Chem. Intermed.*, 2018, **44**, 6419.
18. H. R. Shaterian, N. Fahimi and K. Azizi, *Res. Chem. Intermed.*, 2014, **40**, 1879.
19. S. Azad and B. B. Fatameh Mirjalili, *Res. Chem. Intermed.*, 2017, **43**, 1723.
20. P. K. Sahu, P. K. Sahu, Y. Sharma and D. D. Agarwal, *J. Heterocycl. Chem.*, 2014, **51**, 1193.
21. A. Shaabani, A. Rahmati and S. Naderi, *Bioorg. Med. Chem. Lett.*, 2005, **15**, 5553.
22. N. Basirat, S. S. Sajadikhah and A. Zare, *Res. Chem. Intermed.*, 2020, **46**, 3263.
23. C. Yao, S. Lei, C. Wang, T. Li, C. Yu, X. Wang and S. Tu, *J. Heterocycl. Chem.*, 2010, **47**, 26.
24. N. Shekarlab, R. Ghorbani-Vaghei and S. Alavinia, *Appl. Organomet. Chem.*, 2020, e5918.
25. M. Abedini, F. Shirini, M. Mousapour and O. Goli-Jolodar, *Res. Chem. Intermed.*, 2016, **42**, 6221.
26. X. B. Lu and D. J. Daresbourg, *Chem. Soc. Rev.*, 2012, **41**, 1462.
27. C. Wang, J. Kim, J. Tang, J. Na, Y.-M. Kang, M. Kim, H. Lim, Y. Bando, J. Li and Y. Yamauchi, *Angew. Chem., Int. Ed.*, 2020, **59**, 2066.
28. G. Singh, K. S. Lakhi, S. Sil, S. V. Bhosale, I. Kim, K. Albahily and A. Vinu, *Carbon*, 2019, **148**, 164.
29. Y. Chen, X. Zhang, W. Chen, H. Yang and H. Chen, *Bioresour. Technol.*, 2017, **246**, 101.
30. Y. Li, G. Wang, T. Wei, Z. Fan and P. Yan, *Nano Energy*, 2016, **19**, 165.
31. X. Chen, S. Song, H. Li, G. Gözaydin and N. Yan, *Acc. Chem. Res.*, 2021, **54**, 1711.
32. K. Lee, Y. Jing, Y. Wang and N. Yan, *Nat. Rev. Chem.*, 2022, **6**, 635.
33. M. Ding, X. Liu and J. Yao, *New J. Chem.*, 2021, **45**, 4147.
34. Q. An, C. Liu, S. Deng, Y. Jiao, M. Tang, M. Yang, Z. Ye and B. Zhao, *Chemosphere*, 2022, **304**, 135308.
35. M. Cao, C. Long, S. Sun, Y. Zhao, J. Luo and D. Wu, *J. Energy Inst.*, 2021, **96**, 90.
36. K.-L. Chang, S. C. Muega, B. I. G. Ofrasio, W.-H. Chen, E. G. Barte, R. R. M. Abarca and M. D. G. de Luna, *Chemosphere*, 2022, **291**, 132829.



37 W. Xue, H. Zhao, J. Yao, F. Li and Y. Wang, *Chin. J. Catal.*, 2016, **37**, 769.

38 Z. Dolatkhah, A. Mohammadkhani, S. Javanshir and A. Bazgir, *BMC Chem.*, 2019, **13**, 97.

39 M. Ding, S. Chen, X. Q. Liu, L. B. Sun, J. Lu and H. L. Jiang, *ChemSusChem*, 2017, **10**, 1898.

40 C. Liu, C. Zhang, H. Song, X. Nan, H. Fu and G. Cao, *J. Mater. Chem. A*, 2016, **4**, 3362.

41 S. Tu, Q. Shao, D. Zhou, L. Cao, F. Shi and C. Li, *J. Heterocycl. Chem.*, 2007, **44**, 1401.

